TRASUTA: The Effect of the Structural Rigidity of a Mesocyclic AAZTA-like Chelating Agent on the Thermodynamic, Kinetic, and Structural Properties of Some Divalent Metal and Ga^{3+} Complexes

Ileana Merdzo, Fabio Travagin, Mariangela Boccalon, Enzo Alessio, Luciano Lattuada, Zsolt Baranyai,* and Giovanni B. Giovenzana*

ABSTRACT: Mesocyclic chelating agents such as AAZTA and its derivatives have been recently reported to overcome the relatively low thermodynamic stability of metal complexes of acyclic chelating agents and the slow complexation kinetics of macrocyclic chelating agents. This work reports the preparation of a spirobicyclic hexadentate AAZTA-like chelating agent (TRASUTA) and the investigation of the thermodynamic, kinetic, and structural properties of the corresponding chelates with the PET-relevant Ga^{3+} and selected metal ions. A combination of analytical techniques allowed identification of a coordination isomerization process, involving the coordinating side arms and the inversion of a nitrogen atom and leading to lower thermodynamic and kinetic inertness with respect to mononuclear mesocyclic analogues. The bicyclic system of TRASUTA retains significant dynamics despite the conformational constraint imposed by the spiro-fusion, resulting in a lower stability of the corresponding metal chelates.

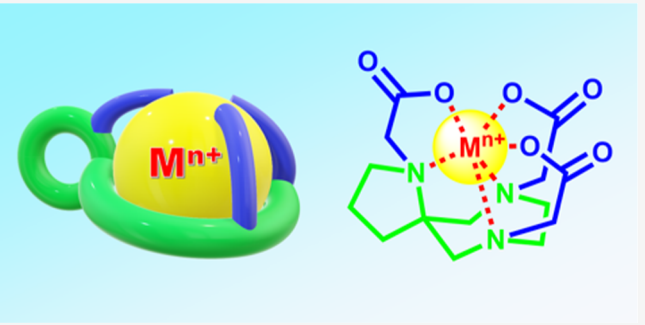

INTRODUCTION

The ability of chelating agents to form complexes with metal ions is widely employed in domestic, agricultural, industrial, and medical applications and witnessed by an impressive annual consumption in the range of hundreds of thousands tons.[1] Medical applications of chelating agents include diagnostics for MRI,[2] PET, and SPECT,[3−5] targeted radiotherapy,[6] and chelation therapy,[7] in which the rapid and selective formation of particularly stable metal complexes is mandatory. High thermodynamic and kinetic stability is usually associated with macrocyclic chelating agents, with the coordinating functional groups preorganized in or onto a large *n*-membered ring ($n \geq 9$).[8] The structural rigidity imposed by some macrocyclic structures takes its toll in the formation kinetics of the metal complex, requiring long times and/or forcing conditions to reach completion, hardly compatible with the often short-lived metal isotopes used in nuclear medicine and with sensitive biomolecules and in vivo conditions.[9] Rapid formation of metal complexes is achieved with acyclic and small (3−6 membered) cyclic chelators, but the thermodynamic and kinetic inertness of these chelates is usually lower, leading to a potential and unwanted loss of the metal ions.

A good compromise between fast complexation kinetics and thermodynamic stability has been achieved with AAZTA, a heptadentate mesocyclic polyaminocarboxylic chelating agent, as well as with its hexadentate derivative DATA^{m}[10] (Figure 1). AAZTA[11] can be easily obtained from inexpensive starting materials, and its complexes with several divalent and trivalent metal ions show good thermodynamic stability associated with fast formation kinetics.[12−15] Owing to these valuable features, several AAZTA-like bifunctional chelating agents[16,17] were synthesized, conjugated to diagnostic-relevant biomolecules, and labeled with metal ions to give a vast array of diagnostic imaging probes.[18−25]

Among them, $^{68}Ga^{3+}$ complexes recently gained a widespread interest as PET contrast agents, culminated in the approval for clinical use by FDA and EMA of ^{68}Ga-edotreotide ([^{68}Ga]-Ga-DOTATOC) to detect somatostatin receptor-positive neuroendocrine tumors.[26]

The slow complexation kinetics associated with DOTA-like macrocyclic chelators led to investigating the possibility of employing AAZTA-based ligands as the chelating moiety in $^{68}Ga^{3+}$-based PET imaging probes due to their prompt formation of the stable chelate. Recent reports demonstrated the superior efficiency in detecting liver and bone metastases of

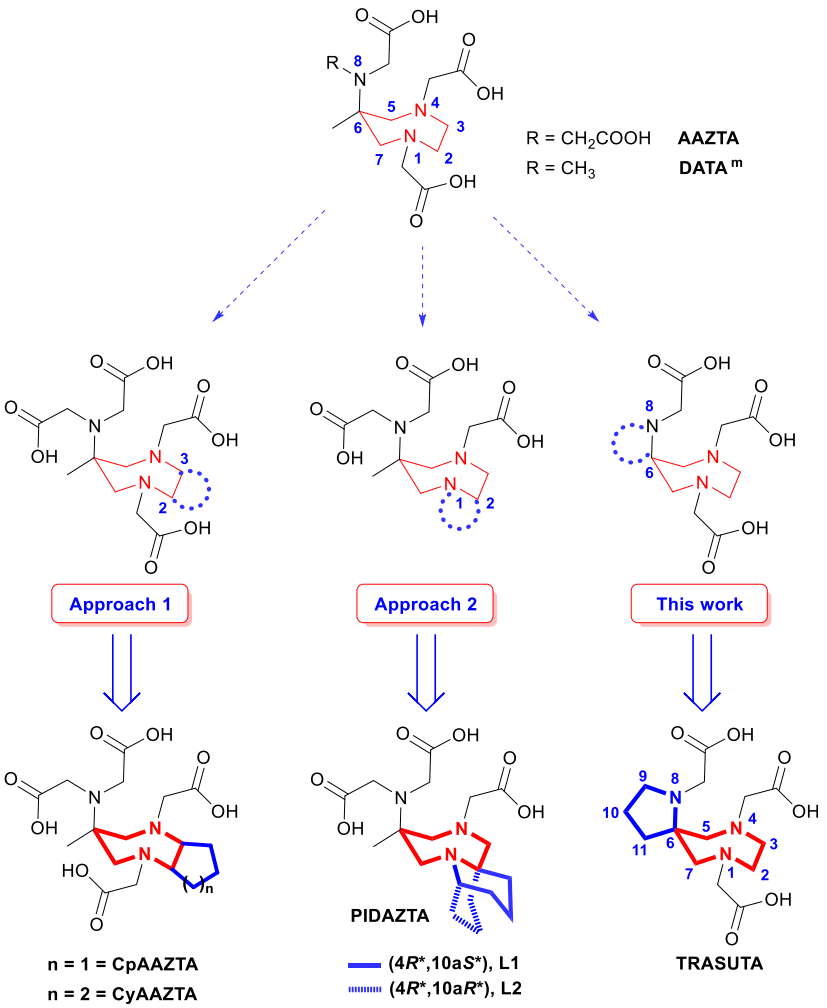

Figure 1. AAZTA and its bicyclic derivatives.

the AAZTA -related [^{68}Ga]Ga-DATA^{5m}-LM4 over the macrocyclic [^{68}Ga]Ga-DOTANOC[27] and the potential of [^{68}Ga]Ga-DATA^{5m}.SA.FAPi for the visualization of cancer-associated fibroblasts of different tumors and metastases thereof.[28]

Prompted by these results, several AAZTA derivatives have been studied in order to improve their coordination properties or (bio)conjugation to molecular targeting vectors.[29] Rigidification of a flexible ligand is commonly undertaken for increasing the stability of its metal complexes. Reducing the conformational freedom of the metal complex generally makes metal release more difficult. Only two different successful approaches to make AAZTA-type ligands more rigid have been reported to date, both involving the formation of bicyclic derivatives.[30−33]

A first approach (#1, Figure 1) is based on the fusion of the C-2/C-3 positions of the diazepane ring with a five- or six-membered ring, providing "CpAAZTA"[30] and "CyAAZTA",[32,33] respectively. A second approach (#2, Figure 1) leads to the "PIDAZTA" stereoisomers (L1 and L2), bearing a six-membered ring fused on N-1 and C-2 of the diazepane ring.[31]

This article focuses on the design and synthesis of a new rigidified spirobicyclic hexadentate AAZTA derivative ("TRASUTA" = H_3L, 1,7,10-**tria**za**spiro**[4.6]-**un**decane-1,7,10-triacetic acid), with a five-membered ring locking C-6 and N-8 (Figure 1).

Herein, we report also a comprehensive investigation of the coordination behavior of TRASUTA toward an array of selected divalent metal ions spanning a range of sizes and hard−soft features (Ca^{2+}, Mn^{2+}, Zn^{2+}, Cu^{2+}, Pb^{2+}, and Cd^{2+}) and the PET-relevant Ga^{3+} ion, aimed at obtaining useful correlations between the structural features of related meso-(bi)cyclic ligands and the thermodynamic and kinetic inertness of the corresponding chelates, to be subsequently translated in the design of improved chelating agents.

EXPERIMENTAL SECTION

Materials. All chemicals employed were of analytical grade. The concentrations of the $CaCl_2$, $MnCl_2$, $Pb(NO_3)_2$, $CdCl_2$, $ZnCl_2$, and $CuCl_2$ stock solutions were determined by complexometric titration against standard Na_2H_2EDTA solutions and *xylenol orange* ($ZnCl_2$, $Pb(NO_3)_2$, $CdCl_2$), murexide ($CuCl_2$), eriochrome black t ($MnCl_2$), and Patton& Reeder ($CaCl_2$) as indicators. The solution of gallium nitrate was prepared by dissolving Ga_2O_3 (99.9%, Fluka) in 6 M nitric acid, followed by evaporation; the residue was then redissolved in a 0.1 M HNO_3 solution. The final concentration of Ga^{3+} was assessed by adding a known excess of standardized Na_2H_2EDTA and back-titration with a standardized $ZnCl_2$ solution. The acid excess of the $Ga(NO_3)_3$ solution was measured by pH potentiometric titration in the presence of excess Na_2H_2EDTA. The concentration and protonation constants of H_3TRASUTA were calculated from the pH-potentiometric titration data obtained with standardized 0.2 M NaOH in the presence and absence of a large (40-fold) excess of $CaCl_2$.

No uncommon hazards are noted.

pH Potentiometry. The stability and protonation constants of the complexes were evaluated from the data obtained by pH-potentiometric titrations of the systems with a 1:1 metal-to-ligand concentration ratio (the concentration of the ligand was generally 0.002 M). A Metrohm 888 Titrando automatic titration workstation with a Metrohm-6.0234.110 combined electrode were used for the pH measurements and titrations. pH potentiometric titrations were performed at a constant ionic strength (0.15 M NaCl) in 6 mL samples at 298 K under magnetic stirring and a N_2 atmosphere. The titrations were carried out in the pH range of 1.7−12.0. For the calibration of the pH meter, KH-phthalate (pH = 4.005) and borax (pH = 9.177) buffers were used. The method reported by Irving et al. was employed[34] for the calculation of $[H^+]$ from the measured pH values. A 0.01 M HCl solution was titrated with the standardized NaOH solution at 298 K in the presence of 0.15 M NaCl ionic strength. Differences (A) of the measured (pH_{read}) and calculated ($-\log[H^+]$) pH values were used to evaluate the equilibrium H^+ concentration from the pH values obtained in the titration experiments (A = 0.015). A waiting time of 60 s between two pH measurements was applied. In the equilibrium calculations, the stoichiometric water ionic product (pK_w) was also used for the calculation of $[OH^-]$ values under basic conditions. The V_{NaOH}—pH_{read} data pairs of the HCl-NaOH titration in the pH range 10.5−12.0 were used for the calculation of the pK_w value (pK_w = 13.80).

Spectrophotometry. The stability constants of [Cu(TRASUTA)]$^-$ were calculated by using the spectrophotometric data of the Cu^{2+}—TRASUTA systems at the absorption band of Cu^{2+} complexes (λ = 400−800 nm) in the $[H^+]$ range of 0.01−1.0 M. In these experiments, the concentrations of Cu^{2+} and H_3TRASUTA were identical ($[Cu^{2+}] = [L] = 0.0016$ M). The adjustment of the H^+ concentration in the samples was performed by the addition of calculated amounts of 3 M HCl. In samples with $[H^+] \leq 0.15$ M, the ionic strength was also maintained constant (I = 0.15 M) by the addition of calculated amounts of NaCl ($I = [Na^+] + [H^+] = 0.15$ M). The samples were stored at 298 K for 1 week. The absorbance of the samples was measured at 615, 635, 655, 675, 695, 715, 735, 755, and 775 nm. The stability and protonation constants of [Cu(TRASUTA)]$^-$ were calculated by using the molar absorptivities of $CuCl_2$, [Cu(TRASUTA)]$^-$, [Cu(HTRASUTA)], and [Cu(H_2TRASUTA)]$^+$, which were determined by recording the Vis spectra of 1.0×10^{-3}, 1.5×10^{-3}, 2.0×10^{-3}, and 2.5×10^{-3} M solutions of $CuCl_2$ and [Cu(TRASUTA)]$^-$ in the pH range of 1.7−7.5. The pH was adjusted by the addition of concentrated NaOH or HCl solutions. The spectrophotometric measurements were carried out with a *PerkinElmer Lambda 365* UV−vis spectrophotometer with 1.0 cm cells at 298 K. The PSEQUAD program[35] was used to calculate the protonation and stability constants.

NMR Experiments. ^{1}H, ^{13}C, and ^{71}Ga NMR spectra were acquired with a *Bruker Avance III* (9.4 T) spectrometer, equipped with *Bruker Variable Temperature Unit* (BVT), *Bruker Cooling Unit*, and a BB inverse z gradient probe (5 mm). The protonation processes of TRASUTA have been investigated by ^{1}H NMR spectroscopy on solutions containing 2.0 mM ligand and 0.15 M NaCl in H_2O (a capillary with D_2O was used for locking). The complexation and protonation processes in the Ga^{3+}—TRASUTA system were followed by ^{1}H and ^{71}Ga NMR spectroscopy at 298 K on solutions containing 2.0 mM aqueous [Ga(TRASUTA)] and 0.15 M NaCl (a capillary with D_2O was used for locking). The pH was adjusted by addition of concentrated NaOH and HCl solutions. The amount of $[Ga(OH)_4]^-$ formed by the decomplexation of [Ga(TRASUTA)] was evaluated by means of the integrals of the ^{71}Ga NMR signal of $[Ga(OH)_4]^-$. The molar integral value of the $[Ga(OH)_4]^-$ complex in the ^{71}Ga NMR spectrum was calculated using 0.001, 0.0015, 0.002, and 0.0025 M solutions of $[Ga(OH)_4]^-$ (pH = 12.5, 0.1 M NaCl, 25 °C). Calculations were carried out using the computer program *Micromath Scientist, version 2.0* (Salt Lake City, UT, USA).

VT ^{1}H and ^{13}C NMR spectra of [Zn(TRASUTA)]$^-$, [Ga(TRASUTA)], [Ga(TRASUTA)OH]$^-$, and [Pb(TRASUTA)]$^-$ were measured on 20 mM samples prepared at pD = 6.46, 4.90, and 7.44 and pH = 7.05 in D_2O and H_2O, respectively. The ^{1}H−^{1}H (COSY) and ^{1}H−^{13}C (HSQC) correlation spectra were collected by standard Bruker pulse programs. Band-shape analyses were performed with the DNMR program of the Bruker Topspin software package. Chemical shift, spin−spin coupling constants, intensity, and LB values under chemical-exchange free condition were fixed as input parameters during the fitting procedure. The similarity of the measured and calculated ^{1}H NMR spectra obtained at different temperature was always greater than 92%.

Transmetalation Reactions. The rates and kinetics of the exchange reactions between [Ga(TRASUTA)OH]$^-$ and Cu^{2+} in the presence of citrate (Cit^{3-}) were investigated by spectrophotometry on the absorption band of the resulting [Cu(TRASUTA)]$^-$ complex (λ = 277 nm). The experiments were carried out with a *PerkinElmer Lambda 365 UV−vis* spectrophotometer in 1.0 cm cells. The concentrations of the [Ga(TRASUTA)OH]$^-$ complex and Cu^{2+} were 0.1, and 0.3, and 0.5 mM in order to ensure pseudo-first-order conditions. [Ga(TRASUTA)OH]$^-$ was prepared just before the experiments by adjusting the pH of the [Ga(TRASUTA)] solution to the required value with concentrated NaOH and HCl solutions. The transmetalation reactions were studied in the presence of large excess of citrate ($[Cit]_t$ = 1.0 mM) to prevent the hydrolysis of Ga^{3+} and Cu^{2+} ions. The exchange rates were determined in the pH range of 6.0−8.0. Constant pH values were maintained by HEPES buffers (0.01 M). Pseudo-first-order rate constants (k_d) were calculated by fitting the absorbance data to eq 1.

$$A_t = (A_0 - A_p)e^{-k_d t} + A_p \quad (1)$$

where A_t, A_0, and A_p are the absorbance values at time t, at the start of the reaction and at equilibrium, respectively. Calculations of the kinetic parameters were made by the fitting of the absorbance−time and relaxation rate−time data pairs to eq 1 with the *Micromath Scientist* computer program (version 2.0, Salt Lake City, UT, USA).

Transchelation Reactions. The ligand-exchange reaction of [Ga(TRASUTA)OH]$^-$ with human serum transferrin (*Sigma*, partially Fe^{3+} saturated) has been followed by spectrophotometry, monitoring the formation of a Ga-transferrin complex at 246 nm and pH = 7.4 with a *PerkinElmer Lambda 365 UV−vis* spectrophotometer. The concentration of the human serum transferrin solution was determined by measuring the absorbance at 280 nm with the use of the molar absorptivity published in the literature (ε_{280} = 91200 cm^{-1} M^{-1}).[36] The temperature was maintained at 298 K, and 0.15 M NaCl ionic strength and 0.025 M $NaHCO_3$ of the samples were kept constant. The Fe^{3+} saturation of the human serum transferrin was determined by spectrophotometric titration of the transferrin solution with $Ga(NO_3)_3$ monitored in the wavelength range of 240−250 nm ($[sTf] = 8.4 \times 10^{-5}$ M, $[Ga^{3+}] = 0-3 \times 10^{-4}$ M, 0.025 M $NaHCO_3$, and 0.15 M NaCl, pH = 7.4, 25 °C, l = 1 mm).

RESULTS AND DISCUSSION

Synthesis. The synthesis of TRASUTA is reported in Scheme 1 and detailed in the Supporting Information. A nitro-Mannich[37] reaction of the commercially available benzathine **1** with aqueous formaldehyde and nitromethane operated in refluxing ethanol led to compound **2** in nearly quantitative yield. Treatment of nitroalcohol **2** with *t*BuOK in dry tetrahydrofuran (rt, 30 min) started a retro-Henry fragmentation with elimination of a formaldehyde molecule. Slow addition of methyl acrylate to the nitronate anion, followed by stirring at room temperature for 3 h, produced the Michael adduct **3** (95% yield over two steps). Catalytic hydrogenation (Raney-Ni, 10 atm of H_2) in methanol (rt, 8 days) reduced the nitro group and triggered the formation of the lactam ring. The catalyst and the solvent were removed by filtration and evaporation, respectively. Toluene was added, and the mixture refluxed for 20 h to complete the cyclization leading to the

Scheme 1. Synthesis of TRASUTA (see the Supporting Information for Details)

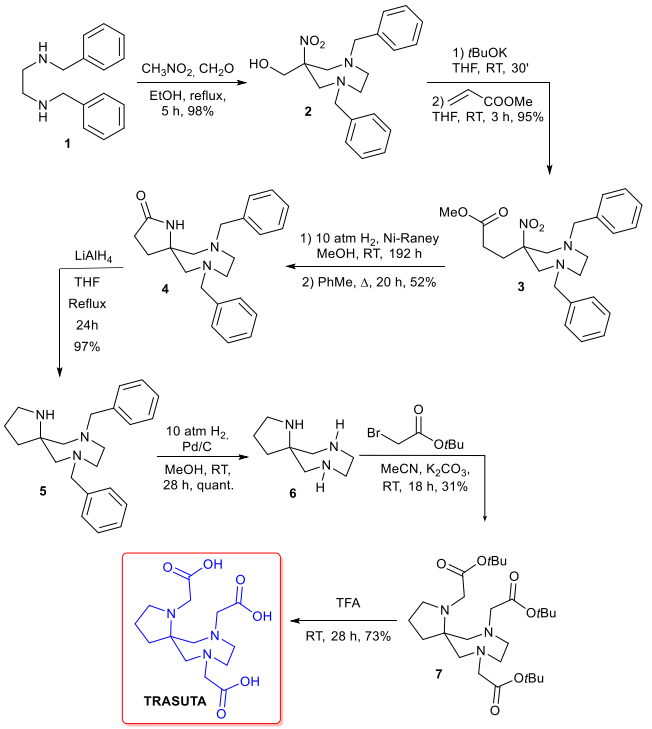

spirolactam **4**, obtained in 52% yield after crystallization from ethyl acetate.

Alternative reduction procedures of the nitro group in compound **3** with either iron or zinc in refluxing acetic acid gave 49 and 15% isolated yield, respectively. Quantitative reduction of the bicyclic lactam **4** to the protected triamine **5** was accomplished by treatment with $LiAlH_4$ in refluxing THF for 1 day under a N_2 atmosphere. Gratifyingly, compound **5** was efficiently debenzylated (H_2, Pd/C, and CH_3OH, r.t., 28 h) yielding triamine **6** in quantitative yield. Exhaustive alkylation of the latter with *tert*-butyl bromoacetate (CH_3CN and K_2CO_3, r.t., 18 h) provided triester **7** in 31% yield. Different combinations of solvents and bases were unsuccessfully tested to improve the yield of the alkylation step. The synthesis of TRASUTA was completed with the deprotection of *t*-butyl ester groups in **7** by treatment with CF_3COOH (r.t., 28 h), leading to the formation of chelating agent in 73% yield (Scheme 1).

Acid−base Properties of TRASUTA. The protonation constants of the TRASUTA ligand (H_3L), defined by eq 2, were determined by pH potentiometry and ^1H NMR spectroscopy. The $\log K_i^H$ values of TRASUTA obtained in 0.15 M NaCl or in 0.15 M $NaNO_3$ solutions are listed in Table 1 (standard deviation is shown in parentheses). The $\log K_i^H$ values determined by ^1H NMR are in good agreement with the values determined by pH-potentiometry.

$$K_i^H = \frac{[H_iL]}{[H_{i-1}L][H^+]} \qquad i = 1, 2 \ldots 5 \tag{2}$$

The comparison of the $\log K_i^H$ values of TRASUTA with those of the hexadentate AAZTA derivatives PIDAZTA (L1 and L2) and DATA^m (Table 1) reveals that the main differences are observed for $\log K_1^H$ and $\log K_2^H$, ascribed to the protonation of the exo- and one of the endocyclic N-atoms, respectively. The first protonation constant is lower, whereas the second one is slightly higher than the related $\log K_i^H$ values of the hexadentate PIDAZTA (L1, L2) and DATA^m. The data in Table 1 also show that the first protonation constant of AAZTA obtained in NaCl solution is lower than that obtained in KCl solution due to the higher stability of the complex with Na^+ compared to K^+.[15,38] The lower affinity of DATA^m and PIDAZTA (L1, L2) toward Na^+, indicated by their higher $\log K_1^H$ values compared to AAZTA, is attributed to the lower denticity.[38] The lower $\log K_1^H$ of TRASUTA compared to those of the hexadentate analogues L1, L2, and DATA^m indicates a higher Na^+ affinity of the TRASUTA ligand, similar to those of the heptadentate ligands CyAAZTA and AAZTA. Consistent with this hypothesis, the $\log K_2^H$ value of TRASUTA is similar to those of CyAAZTA and AAZTA and higher than those of hexadentate DATA^m and PIDAZTA (L1 and L2). The further protonation constants of TRASUTA, taking place on the carboxylic groups, are similar to those of the corresponding $\log K_i^H$ values of DATA^m, PIDAZTA (L1, L2), CyAAZTA, and AAZTA. Finally, the $\Sigma \log K_i^H$ values (Table 1), show that the total basicity of TRASUTA is lower than those of PIDAZTA (L1, L2), CyAAZTA, and AAZTA and higher than that of DATA^m. It is worth noting that the $\log K_i^H$ values of TRASUTA measured in 0.15 M NaCl and $NaNO_3$ are practically identical, indicating that chloride and nitrate do not affect the protonation behavior of TRASUTA. It is commonly accepted that less basic donor groups bind more weakly to metal ions. On this base, TRASUTA is expected to overcome DATA^m (both ligands having three N- and three carboxylate O-donor atoms) in terms of the stability constants of the corresponding metal complexes. However, the size match between the metal ion and the coordination cage, rigidified by the spiro-fusion, must be taken into account.

Complexation Properties of TRASUTA. The stability and protonation constants of M^{n+}—TRASUTA (H_3L)

Table 1. Protonation Constants of TRASUTA, PIDAZTA (L1, L2), DATAm, CyAAZTA, and AAZTA (25 °C)

	TRASUTA			L1[a]	L2[a]	DATA m[b]	CyAAZTA[c]	AAZTA[d]	
I	0.15 M NaCl		0.15 M $NaNO_3$	0.15 M NaCl			0.1 M KCl	0.15 M NaCl	0.1 M KCl
$\log K_1^H$	9.76 (2)	10.30 (3)[e]	10.06 (2)	11.37	11.67	11.51	10.48	10.06	11.23
$\log K_2^H$	6.15 (2)	6.14 (1)[e]	6.15 (2)	5.88	5.22	5.15	6.43	6.50	6.53
$\log K_3^H$	4.14 (2)	3.90 (8)[e]	3.99 (3)	3.56	3.67	3.49	4.23	3.77	3.81
$\log K_4^H$	2.53 (3)	2.50 (9)[e]	2.08 (4)	2.69	3.02	1.30	2.76	2.33	2.26
$\log K_5^H$					1.28		1.68	1.51	1.61
$\Sigma \log K_i x^H$	22.57	22.79[e]	22.27	23.50	24.85	21.45	25.58	24.16	25.44

[a]Ref 31. [b]Ref 38. [c]Ref 33. [d]Ref 13. [e]Obtained by ^1H NMR studies (0.15 M NaCl, 25 °C).

Table 2. Stability and Protonation Constants of the Divalent Metal Ion Complexes with TRASUTA, PIDAZTA (L1, L2), DATA^m, CyAAZTA, and AAZTA Ligands (25 °C)

	TRASUTA	L1[a]	L2[a]	DATA^m[b]	CyAAZTA[c,d]	AAZTA[b,f]
I	0.15 M NaCl				0.1 M KCl	0.15 M NaCl/0.1 M KCl or KNO_3
CaL	**6.67 (6)**	**7.41**	**8.89**	**8.70**	**12.38**	**11.75/12.76**
CaHL	7.42 (6)	6.92	5.62	5.49	4.00	3.41/3.34
MnL	**8.55 (4)**	**11.32**	**12.40**	**11.43**		**14.19/15.44**
MnHL	5.97 (5)	4.02	3.75	3.36		2.61/2.83
ZnL	**12.82 (5)**	**15.11**	**16.13**	**16.54**	**17.09**	**16.02/18.01**
ZnHL	3.76 (3)	3.25	3.66	1.76	4.17	3.95/3.87
ZnH_2L	3.50 (4)	1.97	2.22		2.83	2.53/2.36
$ZnLH_{-1}$	7.87 (3)	11.18	10.54	11.94	9.43	11.36/11.25
CdL[e]	**11.48 (3)**					**17.94**[a]
CdHL[e]	4.22 (3)					3.25[a]
CdH_2L[e]						2.05[a]
PbL[e]	**13.41 (2)**					**19.84**[a]
PbHL[e]	3.71 (4)					3.22[a]
PbH_2L[e]						2.50[a]
CuL[g]	**16.22 (2)**	**18.17**	**19.14**	**18.36**	**20.11**	**20.60/22.27**
CuHL	3.97 (1)	2.99	3.78	3.56	4.24	3.86/3.93
CuH_2L	2.44 (2)	1.51	2.07	1.52	3.08	2.43/2.68
$CuLH_{-1}$	9.35 (6)	11.51	10.30	10.88	9.62	10.62/10.79

[a]Ref 31. [b]Ref 38. [c]Ref 33. [d]Ref 32. [e]25 °C, 0.15 M $NaNO_3$. [f]Ref 15 (25 °C, 0.1 M KCl or KNO_3). [g]By spectrophotometry (I = $[Na^+]$ + $[H^+]$ = 0.15 in the samples where $[H^+] \leq 0.15$ M).

complexes (Ca^{2+}, Mn^{2+}, Zn^{2+}, Pb^{2+}, Cu^{2+}, Cd^{2+}, and Ga^{3+}) are defined by eqs 3 and 4.

$$K_{ML} = \frac{[ML]}{[M][L]} \tag{3}$$

$$K_{MH_iL} = \frac{[MH_iL]}{[MH_{i-1}L][H^+]} \qquad i = 1, 2 \tag{4}$$

The equilibrium constants, displayed in Table 2, were obtained for TRASUTA (H_3L)—M^{n+} complexes by pH-potentiometric and/or UV−vis spectrophotometric measurements (1:1 metal/ligand concentration ratio). The model including the formation at equilibrium of the species ML, MHL, and MH_2L led to the best fitting. The titrimetric data of H_3L obtained with equimolar concentrations of Zn^{2+} and Cu^{2+} show the presence at pH > 7 of an extra base-consuming step, rationalized with the coordination of OH^- (eq 5).

$$K_{M(L)OH} = \frac{[ML]}{[M(L)OH][H^+]} \tag{5}$$

The stability and protonation constants of $[Cu(TRASUTA)]^-$ were determined by spectrophotometry. The equilibrium reaction (eq 6) was studied in the $[H^+]$ range of 0.01−1.0 M (the ionic strength was constant I = $[Na^+]$ + $[H^+]$ = 0.15 in the samples where $[H^+] \leq 0.15$ M), where the presence of Cu^{2+}, [CuHL], $[CuH_2L]^+$, and H_xL species was assumed (x = 4 and 5; y = 2 and 3, eq 6). Some characteristic absorption spectra are shown in Figure S23.

$$Cu^{2+} + H_xL \rightleftharpoons [Cu(H_{x-y}L)] + yH^+ \tag{6}$$

In the absorption spectra of the Cu^{2+}—TRASUTA system, a decrease in the proton concentration results in the increase of the absorbance values, attributable to the progressive formation of the $[Cu(H_2L)]^+$ and [Cu(HL)] species in the $[H^+]$ = 0.01−1.0 M range.

In the pH range of 1.7−12.0, where $[CuL]^-$, [Cu(HL)], $[Cu(H_2L)]^+$, and $[Cu(L)OH]^{2-}$ species are present, the protonation constants of $[Cu(TRASUTA)]^-$ were determined by pH-potentiometric titrations.

The stability constants of Ca^{2+}, Mn^{2+}, Zn^{2+}, Cd^{2+}, Pb^{2+}, and Cu^{2+} complexes formed with TRASUTA are lower by 2−5 log$K$ units than those of the corresponding PIDAZTA, DATA^m, CyAAZTA, and AAZTA complexes. A comparison of the logK_{ML} values of metal complexes formed with the TRASUTA and DATA^m indicates that the stability constants of the DATA^m complexes (Table 2) are generally higher by 2−4 log$K$ units than those of the corresponding complexes of TRASUTA. This finding indicates that the potential ligand rigidification induced by incorporation of the pyrrolidine group in the exocyclic pendant arm does not improve the thermodynamic properties of the TRASUTA complexes with respect to the corresponding DATA^m complexes.

The complexes formed with TRASUTA, as for other AAZTA derivatives, can undergo protonation at low pH; pH potentiometry was used to determine the corresponding protonation constants, listed in Table 2. For $[ZnL]^-$ and $[CuL]^-$ complexes, two protonation constants were determined in the pH range of 2.0−5.0, presumably associated with the protonation of two weakly coordinated carboxylate groups. For the $[CaL]^-$, $[MnL]^-$, $[PbL]^-$, and $[CdL]^-$ complexes, a single protonation step was found that, according to the higher logK_{MHL} values, might take place on one of the carboxylate donor atoms.

Equilibrium Properties of the Ga^{3+}−TRASUTA System. The stability constants of aminopolycarboxylate or aminopolyphosphonate Ga^{3+} complexes have been commonly measured by pH potentiometry following the competition/decomplexation reactions with OH^- at pH > 6.[13,39−41] To determine the stability and protonation constants of the Ga^{3+}−TRASUTA system, the titration was made at a 1:1 metal:ligand concentration ratio.

Table 3. Stability and Protonation Constants of Ga^{3+} Complexes Formed with TRASUTA PIDAZTA (L1, L2), $DATA^m$, CyAAZTA, and AAZTA (25 °C)

	I	GaL	Ga (HL)	Ga (H_2L)	Ga (L)OH	$\log\beta_{Ga(L)OH}$
[Ga(TRASUTA)]	0.15 M $NaNO_3$	17.2 (1)[e]	3.53 (2)	2.38 (3)	5.41 (2) 5.28 (3)[e]	12.2 (1)[e]
[Ga(L1)][a]	**0.15 M NaCl**	**18.77**	2.41		4.04	**14.74**
[Ga(L2)][a]		**21.70**	2.51		3.75	**17.94**
[Ga($DATA^m$)][b]		**21.54**	2.42		6.25	**15.29**
[Ga(CyAAZTA)][c]	**0.1 M KCl**	**21.39**	4.09	2.32	7.31	**14.08**
[Ga(AAZTA)][d]	**0.15 M NaCl**	**21.15**	3.14	1.14	4.60	**16.57**

[a]Ref 31. [b]Ref 38. [c]Ref 33. [d]Ref 13. [e]Obtained by ^{71}Ga NMR spectroscopy at 25 °C in 0.15 M $NaNO_3$ solution.

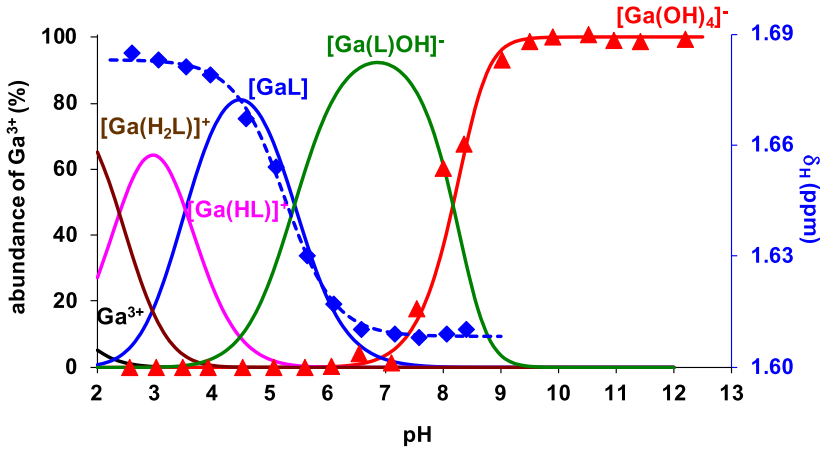

Figure 2. Species distribution in the Ga^{3+}−TRASUTA system. The chemical shift of the overlapping resonances of hydrogen atoms in [Ga(TRASUTA)] (blue ◆, see Scheme 2) and the amount of $[Ga(OH)_4]^-$ (red ▲) were obtained by ^{1}H and ^{71}Ga NMR spectroscopy ($[Ga^{3+}]$ = [TRASUTA] = 2.0 mM, 9.4 T, 0.15 M NaCl, 298 K).

The complexation of Ga^{3+} with TRASUTA and the competition between TRASUTA and OH^- for Ga^{3+} are fast enough to follow the processes by direct pH-potentiometric titration. The optimal fitting of data was achieved with a model including the species [GaL], $[Ga(HL)]^+$, and $[Ga(H_2L)]^{2+}$ at equilibrium. The data also indicate the occurrence of an extra base-consuming process at pH > 4.0, rationalized by assuming the coordination of a hydroxide ion − and the concomitant release of a carboxylate group − with the formation of the $[Ga(L)OH]^-$ species according to eqs 4 and 7

$$Ga^{3+} + L^{3-} + OH^- \rightleftharpoons [Ga(L)OH]^-$$

$$\beta_{Ga(L)OH} = \frac{[Ga(L)OH]}{[Ga^{3+}][L^{3-}][OH^-]} \quad (7)$$

For equilibrium constant calculation, the hydrolysis constants of free Ga^{3+} ions have also been considered ($\log K_{[Ga(OH)]2+}$ = −2.41, $\log K_{[Ga(OH)2]+}$ = −5.92, $\log K_{[Ga(OH)3]}$ = −10.63, and $\log K_{[Ga(OH)4]-}$ = −16.87).[42−44] The stability and protonation constants of the [Ga(TRASUTA)] complex are reported in Table 3, along with the corresponding values for [Ga(L1/L2)], [Ga($DATA^m$)], $[Ga(CyAAZTA)]^-$, and $[Ga(AAZTA)]^-$. The species distribution diagram for the Ga^{3+}—TRASUTA system, calculated on the base of the equilibrium data, is reported in Figure 2.

The stability constant of the [Ga(TRASUTA)] complex ($\log K_{GaL}$ = 17.2, 0.15 M $NaNO_3$, 25 °C) is about 1.5−4.5 log*K* lower than those of [Ga(L1/L2)], [Ga($DATA^m$)], $[Ga(CyAAZTA)]^-$, and $[Ga(AAZTA)]^-$, suggesting that the incorporation of the pyrrolidine group in the exocyclic side chain leads to a slightly less optimal coordination of the Ga^{3+} ion. The cumulative stability constant of the $[Ga(TRASUTA)-OH]^-$ species dominating at pH > 4.0 ($\log\beta_{Ga(L)H-1}$ = 12.2, 0.15 M $NaNO_3$, 25 °C) is the lowest among the Ga^{3+} complexes of AAZTA-like chelating agents. The equilibrium data suggest that the presence of the pyrrolidine group may distort the coordination cage of the AAZTA skeleton, hindering the easy achievement of optimal conformations for the coordination of the amine-N and carboxylate-O donor atoms to Ga^{3+}.

The Ga^{3+}−TRASUTA system was also investigated by ^{1}H and ^{71}Ga NMR in the pH range of 2.0−11.0 (Figures 2, S24, and S25). The integral values of the ^{71}Ga-NMR signal of $[Ga(OH)_4]^-$ (δ_{Ga} = 223 ppm, $\nu_{1/2}$ = 100 Hz, Figure S25) were used to calculate the amount of $[Ga(OH)_4]^-$ formed at pH > 7.0 in the decomplexation of [GaL]. The percentages of $[Ga(OH)_4]^-$ species determined by ^{71}Ga NMR spectroscopy and the distribution of the $[Ga(L)OH]^-$ species obtained by ^{1}H NMR spectroscopy (Figure 2) are in good agreement with the values calculated with the equilibrium data obtained from the pH potentiometric studies.

The species distribution diagrams and the ^{1}H and ^{71}Ga NMR spectra (Figures 2, S24, and S25) reveal that the complexation of Ga^{3+} with TRASUTA is complete at pH ≥ 2.0 and the species [Ga(TRASUTA)] dominates in the pH range of 4−5. However, the ^{71}Ga NMR signal in [Ga(TRASUTA)] is broad (Figure S25) and basically undetectable, which can be explained by the fact that ^{71}Ga is quadrupolar, so the line width is strongly dependent on the symmetry of the Ga^{3+} complex, and the Ga^{3+} ion in [Ga(TRASUTA)] is in a less-symmetric coordination environment. The ^{1}H NMR spectra of the Ga^{3+}-TRASUTA system are complex with several overlapping

Scheme 2. Dissociation Mechanism of $[Ga(TRASUTA)OH]^-$

Table 4. Rate (k_i), Equilibrium Constants (K_i), and Half-Life Values ($t_{1/2} = \ln 2/k_d$) for the Dissociation of the Ga^{3+} Complexes with Mesocyclic Chelating Agents (298 K) in the Presence of Cu^{2+}

	TRASUTA	PIDAZTA (4aR*,10aS*)[31] (L1)	PIDAZTA (4aR*,10aR*)[31] (L2)	$DATA^m$[38]	CyAAZTA[33]	AAZTA[13]
I	0.15 M NaCl				0.1 M KCl	
k_0/s^{-1}	$(2.3 \pm 0.1) \times 10^{-4}$	1.4×10^{-4}	4.3×10^{-7}	8.0×10^{-6}	1.7×10^{-5}	3.0×10^{-6}
$k_{OH}/M^{-1}\ s^{-1}$	2100 ± 100		0.6	31	68	10
$K_{Ga(L)OH}/M^{-1}$	2.4×10^5	1.1×10^4	5.6×10^3	1.8×10^6	2.0×10^7	5.2×10^4
k_d/s^{-1} (pH = 7.4)	1.1×10^{-3}	7×10^{-4}	6.5×10^{-7}	1.7×10^{-5}	2.3×10^{-5}	9.2×10^{-6}
$t_{1/2}/h$ (pH = 7.4)	**0.18**	**0.27**	**295**	**11.2**	**8.5**	**21**

multiplets (Figure S24). The deprotonation of the residual $[Ga(HTRASUTA)]^+$ and the formation of $[Ga(TRASUTA)OH]^-$ at 5 < pH < 7.5 result in a modest upfield shift of all ^1H NMR signals. Based on the upfield shift of the ^1H NMR signals, it might be assumed that the deprotonation of $[Ga(HTRASUTA)]^+$ might occur at one weakly and/or noncoordinated carboxylate group of TRASUTA. On the other hand, the formation of $[Ga(TRASUTA)OH]^-$ presumably takes place by the replacement of a coordinated COO^- group with hydroxide ions in the coordination sphere. Similar phenomena have been observed in the Ga^{3+}−$DATA^m$ and Ga^{3+}−AAZTA systems.[13,38] At pH > 7.5, competition between TRASUTA and OH^- for Ga^{3+} is confirmed by the formation of $[Ga(OH)_4]^-$ (Figure S25) and free TRASUTA (Figure S24). The slight upfield shift of ^1H NMR resonances of free TRASUTA compared to the spectrum in D_2O (Figure S14) is explained by the deprotonation of the HL^{2-} species leading to the fully deprotonated L^{3-} species at pH > 8.2 (Figure S24).

Transmetalation Kinetics of the $[Ga(TRASUTA)OH]^-$ Complex with Cu^{2+}. The kinetic inertness of metal chelates for in vivo applications as radiopharmaceuticals must be assessed to ensure the delivery of the radioisotope as an intact complex to the target tissue. Although Ga^{3+} chelates are usually associated with relatively high thermodynamic stability and kinetic inertness, body fluids contain an excess of competing endogenous species either in the form of powerful ligands (e.g., transferrin) or of metal ions (e.g., Zn^{2+} and Cu^{2+}), potentially leading to the transchelation or transmetalation of the administered Ga^{3+} chelates.[13,15,31,33,38]

The dissociation yield of a Ga^{3+} chelate is a function of the stability constants of the different complexes formed with competing endogenous species. According to the equilibrium data (Table 2), the endogenous metal ions (mainly Cu^{2+} and Zn^{2+}) and transferrin (Tf) may take a part in the exchange reactions of $[Ga(TRASUTA)OH]^-$ which starts to be predominant at pH ≥ 5.5 (Figure 2), with the release of Ga^{3+} and the formation of Ga(Tf) and Ga_2(Tf) complexes ($\log K_{GaTf}$ = 18.88 and $\log K_{Ga2(Tf)}$ = 17.65).[45] The kinetic properties of Ga^{3+} chelates are usually determined under strongly acidic and basic conditions ($[H^+]$ > 1.0 M and $[OH^-]$ > 0.1 M, respectively).[46−48] To approach physiological conditions, the kinetic stability of $[Ga(TRASUTA)OH]^-$ was determined by spectrophotometry, following the exchange reactions of the Ga^{3+} complex with Cu^{2+} in the presence of excess Cu^{2+} and of citrate (Cit) to prevent hydrolysis of free Ga^{3+} and Cu^{2+} ions in the pH range of 6.0−8.0 (Figure S26). The k_d pseudo-first-order rate constants of the transmetalation reaction of $[Ga(TRASUTA)OH]^-$ (Figure S27) indicate that the rate of the exchange reaction is directly proportional to the concentration of OH^-, but it does not depend on $[Cu^{2+}]$ and [Cit] (the increase of $[Cu^{2+}]$ in the presence of constant $[Cit]_{tot}$ results in the formation of more $[Cu(Cit)H_{-1}]^{2-}$ species and the decrease of $[Cit]_{free}$ in the pH range of 6.0−8.0). By taking into account the kinetic data, we can assume that the reactions of $[Ga(TRASUTA)OH]^-$ occur through two parallel dissociation pathways, the spontaneous (k_0) and the OH^- ion-assisted (k_{OH}) dissociation (Scheme 2), followed by a fast reaction between free TRASUTA and the Cu^{2+} ions. The rate and protonation constants of the transmetalation reaction of $[Ga(TRASUTA)OH]^-$ with Cu^{2+} are reported in Table 4 along with those of $[Ga(PIDAZTA)OH]^-$, $[Ga(DATA^m)OH]^-$, $[Ga(CyAAZTA)OH]^{2-}$, and $[Ga(AAZTA)OH]^{2-}$. Experimental details, definitions, and equations used for the evaluation of the kinetic data are summarized in the Supporting Information.

The kinetic data in Table 4 show that the k_0 rate constant of the spontaneous dissociation of $[Ga(TRASUTA)OH]^-$ is about 2, 540, 29, 14, and 77 times higher than those of the $[Ga(L1))OH]^-$, $[Ga(L2)OH]^-$, $[Ga(DATA^m)OH]^-$, $[Ga(CyAAZTA)OH]^{2-}$, and $[Ga(AAZTA)OH]^{2-}$ complexes, respectively. The spontaneous demetalation of the $[Ga(L)OH]^-$ species may take place by the rearrangement of the coordinated donor atoms, triggering the fission of metal ion-donor atom bonds and the concomitant release of the Ga^{3+} ion.

The exchange reaction of $[Ga(TRASUTA)OH]^-$ with Cu^{2+}, that occurs through the OH^--assisted dissociation (k_{OH}) path, has a rate constant (k_{OH}) that is about 3500, 68, 31, and 210 times higher than the corresponding k_{OH} of $[Ga(L2)OH]^-$, $[Ga(DATA^m)OH]^-$, $[Ga(CyAAZTA)OH]^{2-}$, and $[Ga(AAZTA)OH]^{2-}$, respectively. The OH^--assisted dissociation of $[Ga(L)OH]^-$ species presumably takes place through the replacement of another coordinated COO^- donor group by a hydroxide ion, generating the labile $[Ga(L)(OH)_2]^{2-}$ intermediate, the latter rapidly releasing the Ga^{3+} ion, thus explaining the significantly larger rate constant of the OH^--assisted dissociation pathway. By considering the above-mentioned equilibrium and rate constants, the rate and the half-life ($t_{1/2} = \ln 2/k_d$) of the dissociation reactions of $[Ga(TRASUTA)OH]^-$ were calculated close to physiological

conditions (pH = 7.4, 25 °C) and compared with the corresponding values of Ga^{3+} complexes formed with L1, L2, $DATA^m$, CyAAZTA, and AAZTA (Table 4). The calculated dissociation half-life of $[Ga(TRASUTA)OH]^-$ at pH = 7.4 is about 1.5, 1640, 62, 47, and 117 times shorter than those of $[Ga(L1)OH]^-$, $[Ga(L2)OH]^-$, $[Ga(DATA^m)OH]^-$, $[Ga(CyAAZTA)OH]^{2-}$, and $[Ga(AAZTA)OH]^{2-}$, respectively, due to the faster spontaneous and OH^--assisted Ga^{3+}-release pathways. The lower $t_{1/2}$ value of $[Ga(TRASUTA)OH]^-$ highlights that the fusion of the pyrrolidine ring with the exocyclic pendant moiety of the AAZTA ligand results in a $[Ga(L)OH]^-$ species with significantly lower inertness under physiological conditions.

Transchelation Kinetics of the $[Ga(TRASUTA)OH]^-$ Complex with Human Serum Transferrin. Transferrins are well-known Fe^{3+}-transporting proteins. On the base of their biological function, three types of transferrin are identified: serum transferrin (sTf), lactoferrin (LTf), and ovotransferrin (OTf).[49] Transferrins are ~80 kDa single-chain bilobal glycoproteins with one Fe^{3+}-binding site in each lobe. Both sTf and LTf interact strongly with Ga^{3+} ions ($\log K_{GaTf}$ = 18.88 and $\log K_{Ga2Tf}$ = 17.65) due to the similar coordination behavior of Ga^{3+} and Fe^{3+} ions.[45] Since sTf is generally only partially saturated with Fe^{3+}, it retains a relatively high capacity to bind other metal ions, like Ga^{3+}. The saturation of human sTf with Fe^{3+} was determined by titrating a solution of sTf (8.4×10^{-5} M) with $Ga(NO_3)_3$ ($0-3 \times 10^{-4}$ M). The exchange reaction between Ga^{3+} and the coordinated Fe^{3+} ions of sTf is neglected due to the large difference between the stability constants of the corresponding complexes.[45,49] All titrations were made in the presence of $NaHCO_3$ (25 mM) at pH = 7.4 and 298 K. The absorption spectra of the $Ga^{3+}-$sTf system are shown in Figure S28, and the plot of absorbance as a function of $[Ga^{3+}]/[sTf]$ are shown in Figures S28 and S29. The increase in absorbance at 246 nm as a function of $[Ga^{3+}]/[sTf]$ (Figure S29) reflects the binding of Ga^{3+} at the iron-binding sites of sTf. The saturation curves reach a plateau at about $[Ga^{3+}]/[sTf] \approx 1.5$. The intersection of absorbance values vs $[Ga^{3+}]/[sTf]$ in Figure S29 ($[Ga^{3+}]/[sTf] = 1.53$) reveals that the saturation of human sTf with Fe^{3+} is 23.5%, close to the physiological saturation of sTf (ca. 30%).[45]

To investigate the extent and the rate of the competition reactions between TRASUTA and transferrin, the ligand-exchange reaction between the $[Ga(TRASUTA)OH]^-$ complex and sTr was followed by spectrophotometry at the absorption band of the $Ga^{3+}-$sTf complex in the 240–250 nm range (eq 8 and Figure 3).

$$[Ga(TRASUTA)OH]^- + sTf \rightleftharpoons Ga(sTf) + TRASUTA \quad (8)$$

The rates of the ligand-exchange reaction were studied in the presence of a high excess of $[Ga(TRASUTA)OH]^-$ ($[Ga(TRASUTA)OH]^-$ = 0.1 mM, [sTf] = 20 μM, pH = 7.5, 25.0 mM $NaHCO_3$, 0.15 M NaCl, 298 K). The rate of the transchelation reactions between $[Ga(AAZTA)OH]^{2-}$, $[Ga(DATA^m)OH]^-$, $[Ga(L1)OH]^-$, and $[Ga(L2)OH]^-$ chelates and human sTf were investigated in the presence of various concentration of Ga^{3+} complexes and human sTf.[13,31,38] In these experiments, Ga^{3+} complexes were applied in a large excess with respect to [sTf] to ensure pseudo-first order conditions. These kinetic experiments reveal that the rate of the reactions was independent of [sTf] and increases with the concentration of the Ga^{3+} complexes, which can be explained by a rate-determining dissociation of the Ga^{3+} complexes, followed by a rapid reaction between the Ga^{3+} and human sTf. Based on analogy, it is assumed that the rate of the transmetalation between $[Ga(TRASUTA)OH]^-$ and human sTf is independent of the [sTf] and increases with the concentration of the Ga^{3+} complex. The ligand-exchange reaction in such a condition can be considered as a pseudo-first-order process and, consequently, the reaction rate is expressed with eq S3. Keeping in mind the molar absorptivity of Ga(sTf) (ε_{246} = 14758 cm^{-1} M^{-1}), the rate constants (k_d) were calculated from the slope of the kinetic curve ($\Delta Abs/\Delta t$, inset of Figure 3) with eq 9. The slope of the kinetic curve has been considered to be up to 40% conversion in order to be sure of the Ga(sTf) complex formation. The rate constant (k_d) obtained at 20 μM human sTf concentration was 2.0×10^{-3} s^{-1}.

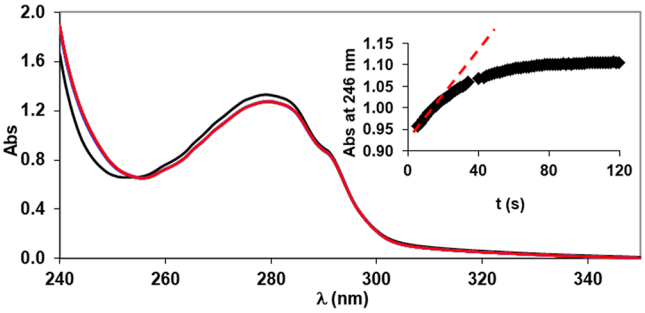

Figure 3. Absorption spectra of the $[Ga(TRASUTA)OH]^-$ — sTf system. [$[Ga(TRASUTA)OH]^-$ = 1.0×10^{-4} M, [sTf] = 2.0×10^{-5} M, pH = 7.5, 25.0 mM $NaHCO_3$, 0.15 M NaCl, 298 K, l = 0.875 cm.

$$k_d = \frac{\Delta Abs}{dt} \times \frac{1}{\varepsilon_{Ga(sTf)}} \times \frac{1}{[GaL]_t} \quad (9)$$

In our experimental conditions, the rate of the formation of the Ga(sTf) adduct by the reaction of the free Ga^{3+} ion and sTf is about 2–3 times faster than that of the transchelation reaction between $[Ga(TRASUTA)OH]^-$ and sTf. The rate-determining step of the transchelation between $[Ga(TRASUTA)OH]^-$ and sTf is the dissociation of the $[Ga(TRASUTA)OH]^-$ complex. The k_d rate constants characterizing the ligand-exchange reaction of $[Ga(TRASUTA)OH]^-$ with sTf ($k_d = 2.0 \times 10^{-3}$ s^{-1}) and the metal-exchange reaction between $[Ga(TRASUTA)OH]^-$ and Cu^{2+} in the presence of citrate ($k_d = 1.1 \times 10^{-3}$ s^{-1}) at pH = 7.4 and 25 °C in 0.1 M NaCl are practically equal. On the base of these results, human sTf has no effect on the rate of dissociation, the latter taking place through the spontaneous and hydroxide-assisted dissociations of $[Ga(TRASUTA)OH]^-$, followed by a fast reaction between the released Ga^{3+} ions and human sTf.

Solution Structure of the $[Zn(TRASUTA)]^-$, $[Ga(TRASUTA)]$, $[Ga(TRASUTA)OH]^-$, and $[Pb(TRASUTA)]^-$ Complexes. To acquire a deeper insight into the structural properties of $[M(TRASUTA)]^{0,1-}$ complexes, the solution structures of $[Zn(TRASUTA)]^-$, $[Ga(TRASUTA)]$, $[Ga(TRASUTA)OH]^-$, and $[Pb(TRASUTA)]^-$ were investigated by multinuclear NMR spectroscopy. 1D/2D NMR spectra of Zn^{2+}, Ga^{3+}, and Pb^{2+} complexes with TRASUTA obtained at 298–353 K, are shown in Figures 4 and 5, as well as in Figures S30–S48. The structure and the possible isomerization of

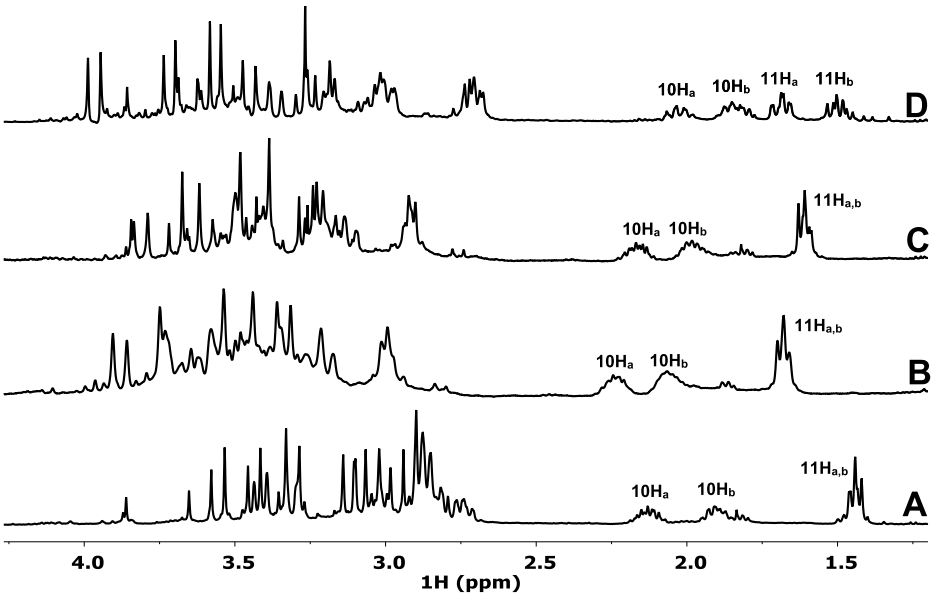

Figure 4. ^{1}H NMR spectra of [Zn(TRASUTA)]$^{-}$ (A), [Ga(TRASUTA)]$^{-}$ (B), [Ga(TRASUTA)OH]$^{-}$ (C), and [Pb(TRASUTA)]$^{-}$ (D) ([ML] = 20 mM, pD = 6.46 (ZnL), 4.9 (GaL), and 7.44 (GaLOH) and pH = 7.05, 9.4 T, 298 K, D_2O).

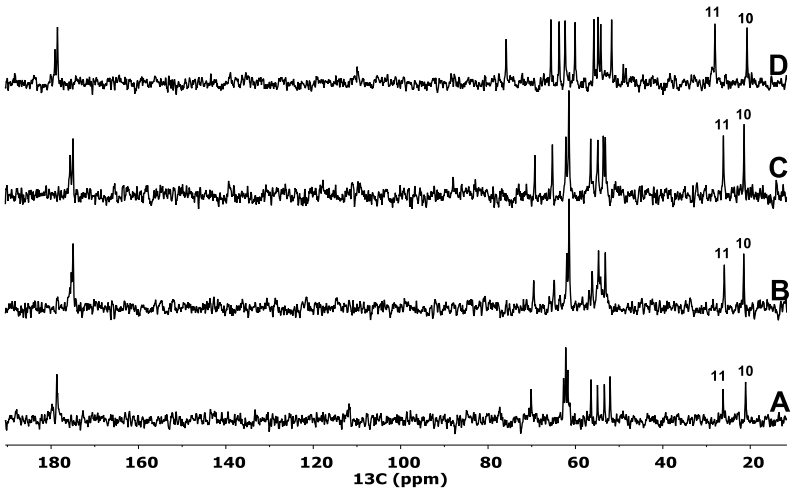

Figure 5. ^{13}C NMR spectra of [Zn(TRASUTA)]$^{-}$ (A), [Ga(TRASUTA)]$^{-}$ (B), [Ga(TRASUTA)OH]$^{-}$ (C), and [Pb(TRASUTA)]$^{-}$ (D) ([ML] = 20 mM, pD = 6.46 (ZnL), 4.9 (GaL), and 7.44 [Ga(L)OH] and pH = 7.05 (PbL), 9.4 T, 298 K, D_2O).

[M(TRASUTA)]$^{0,1-}$ with the assignment of selected ^{1}H and ^{13}C NMR signals are shown in Scheme 3.

Multinuclear NMR studies of [Zn(TRASUTA)]$^{-}$, [Ga(TRASUTA)]$^{-}$, [Ga(TRASUTA)OH]$^{-}$, and [Pb(TRASUTA)]$^{-}$ indicate that these complexes have C_1 symmetry in solution. It could be assumed that the structures of [Zn(TRASUTA)]$^{-}$ and [Ga(TRASUTA)]$^{-}$ are quite similar to that reported for [Ga(DATA^{m})] in the solid state,[38,50] in which the Ga^{3+} ion is coordinated in a distorted octahedral geometry by the N_3O_3 donor set of the chelating agent. The exocyclic N atom, one endocyclic N atom, the exocyclic COO^{-}, and one of the ring-COO^{-} atoms bind the Ga^{3+} ion in the equatorial positions. The remaining endocyclic N atom and ring-COO^{-} occupy the axial positions of the Ga^{3+} ion.[50] Single crystals of [Ga(DATA^{m})] contain enantiomeric Ga^{3+} complexes with opposite conformations of the ring and helicities of the acetate pendant arms. Based on the torsion angle values, the conformation of the seven-membered ring is close to that of the twisted-chair found in the single crystal of the free AAZTA ligand.[51] In all the isomers of [Ga(DATA^{m})], two acetate pendant arms have the same helicities, whereas the third acetate arm has the opposite orientation. The ^{1}H NMR spectrum of the [Ga(DATA^{m})] complex shows two singlets for

Scheme 3. Structural Interconversion Process in [M(TRASUTA)]$^{0,1-}$ Complexes (M^{n+} = Zn^{2+}, Ga^{3+}, and Pb^{2+}; Charges Omitted for Clarity)

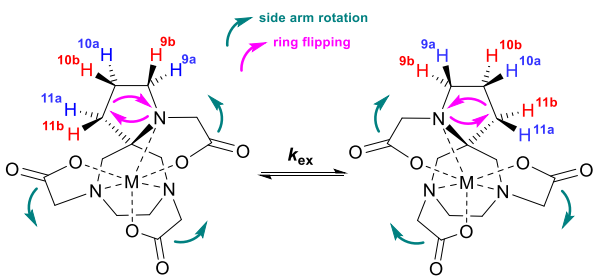

Table 5. Rate Constants and Activation Parameters for the Interconversion Process in the $[Zn(TRASUTA)]^-$, [Ga(TRASUTA)], and $[Ga(TRASUTA)OH]^-$ Complexes

	$[Zn(TRASUTA)]^-$	[Ga(TRASUTA)]	$[Ga(TRASUTA)OH]^-$
$\Delta H^{\ddagger}$/kJ·mol^{-1}	13.6 ± 0.6	14.2 ± 0.9	19 ± 1
$\Delta S^{\ddagger}$/J·mol^{-1}·K^{-1}	−179 ± 2	−176 ± 5	−164 ± 7
$\Delta G^{\ddagger}_{298}$/kJ·mol^{-1}	**66.9**	**66.6**	**68.2**
k_{ex}^{298}/s^{-1}	**11.4**	**12.9**	**6.7**

the methyl groups (on C6 and N_{exo}), whereas the remaining protons are all diastereotopic, with 5 AB-doublets for C5, C7, and for the side arms methylene protons and an AA'BB' multiplet for the C2−C3 annular ethylene moiety (Figure 1).[50] The ^{1}H NMR studies of the $[Ga(DATA^m)]$—$[Ga(DATA^m)OH]^-$ systems also reveal that the formation of $[Ga(DATA^m)OH]^-$ in the pH range of 4.0−8.0 results in the upfield shifts of the N_{exo}-CH_3 and C−CH_3 singlets, reasonably attributed to the hydroxide ion replacing one ring-COO^- group in the coordination sphere of the metal ion. In addition, the ^{1}H NMR signals of the $[Ga(DATA^m)OH]^-$ species are broader than those of $[Ga(DATA^m)]$ presumably due to the significantly higher flexibility of the five-coordinated ligand in $[Ga(DATA^m)OH]^-$. The exchange between $[Ga(DATA^m)]$ and $[Ga(DATA^m)OH]^-$ complexes is slow on the NMR time scale at 273 K (the singlets of N_{exo}−CH_3 and C−CH_3 protons of the two species collapse at $T \geq 298$ K).[38]

The ^{1}H and ^{13}C NMR spectra of the $[M(TRASUTA)]^{0,1-}$ complexes (M^{n+} = Zn^{2+}, Ga^{3+}, and Pb^{2+}) obtained at 298 K (Figures 4, 5, S30, S31, S35, S36, S40, S41, S45, and S46) contain one set of signals, consistent with the presence of a single species in solution. The ^{1}H resonances of the 10 methylene protons in $[M(TRASUTA)]^{0,1-}$ are sharp up to 313 K, with only a modest upfield shift. The ^{1}H and ^{13}C NMR signals of the $[Pb(TRASUTA)]^-$ complex remain practically unchanged up to 343 K (Figures S45 and S46). This can be explained by a strong interaction between the N donor atoms of TRASUTA and soft Pb^{2+}, resulting in the hindrance of the intramolecular rearrangement (Scheme 3). Since the ^{13}C NMR spectra of the $[M(TRASUTA)]^-$ complexes remain unchanged up to 353 K (Figures S31, S36, S41, and S46), it can be assumed that the dissociation of the Zn^{2+}, Ga^{3+}, and Pb^{2+} complexes does not take place with the release of the free TRASUTA ligand. In the VT ^{1}H NMR spectra of $[Zn(TRASUTA)]^-$, $[Ga(TRASUTA)]^-$, and $[Ga(TRASUTA)OH]^-$, the ^{1}H resonances gradually broaden upon increasing the temperature, especially those of the ^{1}H NMR signals of the $10H_{a,b}$ and $11H_{a,b}$ protons of the pyrrolidine group, possibly due to exchange between respective mutual positions in each pair of diastereotopic protons, *via* a process involving the acetate arm rotation and the ring flipping with inversion of the amino N donor atom (either stepwise or concerted, Scheme 3). Since the ^{1}H and ^{13}C NMR spectra of $[Zn(TRASUTA)]^-$, $[Ga(TRASUTA)]^-$, and $[Ga(TRASUTA)OH]^-$ contain only one set of signals, it can be assumed that the motion of the carboxymethyl pendant arms and the flipping of the N donor atom result in the interconversion between the two enantiomers of each complex. The motion of the carboxymethyl pendant arms and the flipping of the N donor atom might occur simultaneously or in subsequent steps. Similar phenomena have been observed by NMR for the axial—equatorial exchange of the acetate arms in $[Zn(EDTA)]^{2-}$, $[Pb(EDTA)]^{2-}$, $[Al(EDTA)]^-$, $[Ga(EDTA)]^-$, and $[In(EDTA)]^-$ complexes.[52−54] The ^{1}H NMR signals of the $11H_{a,b}$ protons of $[Zn(TRASUTA)]^-$, [Ga(TRASUTA)], and $[Ga(TRASUTA)OH]^-$ were chosen for line-shape analysis, simulating the ^{1}H NMR spectra in the temperature range of 298−353 K (Figures S34, S39, and S44). The NMR spectral parameters for the resonances of $10H_{a,b}$ and $11H_{a,b}$ protons in $[Zn(TRASUTA)]^-$, [Ga(TRASUTA)], $[Ga(TRASUTA)OH]^-$, and $[Pb(TRASUTA)]^-$ complexes are summarized in Table S1. The activation parameters (Table 5) for the interconversion process in $[Zn(TRASUTA)]^-$, [Ga(TRASUTA)], and $[Ga(TRASUTA)OH]^-$ have been estimated with the Eyring equation by using the k_{ex} rate constant obtained by the line-shape analysis (Figure S49).

The activation enthalpy ($\Delta H^{\ddagger}$) and entropy ($\Delta S^{\ddagger}$) values characterizing the interconversion process in $[Zn(TRASUTA)]^-$ and [Ga(TRASUTA)] are very similar and smaller than those of $[Ga(TRASUTA)OH]^-$. These data indicate that the motion of the carboxymethyl pendant arms and the flipping of the N donor atom in the pyrrolidine ring are slower in $[Ga(TRASUTA)OH]^-$ than in $[Zn(TRASUTA)]^-$ and [Ga(TRASUTA)]. Based on this experimental finding, the formation of $[Ga(TRASUTA)OH]^-$ with the substitution of the ring acetate group of [Ga(TRASUTA)] by OH^- resulted in a more favorable accommodation of Ga^{3+} in the coordination environment of TRASUTA. Surprisingly, the activation enthalpy values of the interconversion process are relatively low for all the investigated species. However, the negative and rather large activation entropy values, which can be explained by the formation of a temporarily ordered transition state, indicate that the interconversion process is mainly entropy-controlled.

According to the result of the detailed NMR studies and theoretical calculations, the exchange between axial and equatorial carboxymethyl arms in $[Zn(EDTA)]^{2-}$, $[Pb(EDTA)]^{2-}$, $[Al(EDTA)]^-$, $[Ga(EDTA)]^-$, and $[In(EDTA)]^-$ chelates may take place by two distinct routes: (i) *direct exchange*, which might take place through the complete dissociation of the whole iminodiacetate moiety, followed by the N atom inversion[52,53] and (ii) *indirect rearrangement*, involving several reversible elementary steps and the formation of heptacoordinated intermediates.[54] DFT calculations revealed that in the $[Al(EDTA)]^-$ complex, the complete displacement of the carboxymethyl groups out from the first coordination sphere of the Al^{3+} ion is characterized by very high activation free energy ($\Delta G^{\ddagger}_{298}$ = 125 kJ·mol^{-1}).[54] Conversely, the formation of the heptacoordinated $[Al(EDTA)(H_2O)]^-$ species requires significantly lower activation energy (the binding energy of H_2O in $[Al(EDTA)(H_2O)]^-$ is about 32 kJ·mol^{-1}), and the presence of H_2O in the inner-sphere of Al^{3+} results in the weakening of the Al−O^- and Al−N bonds, which may facilitate the decoordination of the acetate arm and the inversion of the N donor atom.[54] This theory is confirmed by the X-ray structure of $[Zn(CDTA)]^{2-}$ in $[\{Zn(H_2O)_5\}\{Zn(CDTA\}]\cdot H_2O$ and $[Zn(CDTA)(H_2O)]^{2-}$ in $[\{Zn(H_2O)_4\}\{Zn(CDTA)(H_2O)\}]\cdot 4H_2O$. In

$[Zn(CDTA)]^{2-}$, the Zn^{2+} ion is hexacoordinated with two N and two carboxylate O donor atoms in the equatorial positions, and by two other carboxylate O donor atoms in axial positions which complete the coordination sphere in a distorted octahedral geometry. In $[Zn(CDTA)(H_2O)]^{2-}$, the Zn^{2+} ion is pseudoheptacoordinated in a monocapped trigonal prism geometry. Importantly, the seventh donor atom is a water oxygen and an in-plane carboxylate oxygen donor atom has a distance of 3.135 Å from the Zn^{2+} ion.[55,56]

Based on analogy, it can be assumed that the interconversion process in the $[Zn(TRASUTA)]^-$, [Ga(TRASUTA)], and $[Ga(TRASUTA)OH]^-$ complexes might similarly occur by the formation of the heptacoordinated $[M(L)H_2O]^{0,1-}$ species that might also provide a rational explanation for the large negative value of the activation entropy. In the heptacoordinated $[M(L)H_2O]^{0,1-}$ species, the displacement of the acetate group and the inversion of the N donor atom are likely followed by the substitution of the inner-sphere H_2O with the O^- donor atom of the acetate group.

CONCLUSIONS

This article reports the preparation of a new hexadentate spirobicyclic chelating agent (H_3TRASUTA) and the investigation of the thermodynamic properties of the corresponding Ca^{2+}, Mn^{2+}, Zn^{2+}, Cu^{2+}, Pb^{2+}, Cd^{2+}, and Ga^{3+} complexes. For the Ga^{3+} complex, in-depth kinetic investigations were also performed. Finally, the structural features and dynamic behavior of the Zn^{2+}, Pb^{2+}, and Ga^{2+} complexes with TRASUTA were assessed.

TRASUTA is devised to study the effect of the conformational constraint imposed by the spirobicyclic structure on the stability of the corresponding metal chelates. Quite surprisingly, the presence of the spiro-fused bicyclic system does not increase the stability and the inertness of the metal complexes. The thermodynamic stability of selected metal complexes of TRASUTA is slightly lower than the corresponding chelates with the structurally related flexible ligand $DATA^m$. Moreover, the kinetic inertness of Ga^{3+}—TRASUTA is about 10 times lower than that of Ga^{3+}—$DATA^m$ due to the lability of the $[Ga(L)OH]^-$ species dominating under physiological conditions.

The structural features and the dynamic behavior of the $[Zn(TRASUTA)]^-$, $[Pb(TRASUTA)]^-$, [Ga(TRASUTA)], and $[Ga(TRASUTA)OH]^-$ complexes were determined by multinuclear variable-temperature NMR studies. The dynamics of the Zn^{2+}– and Ga^{3+}–TRASUTA complexes in solution are dominated by a coordination isomerization involving the side arms and the concomitant inversion of the exocyclic nitrogen atom. In $[Zn(TRASUTA)]^-$, [Ga(TRASUTA)], and $[Ga(TRASUTA)OH]^-$, the isomerization processes is entropy controlled, and on the basis of the highly negative entropy values, it is assumed to take place by the formation of heptacoordinated $[M(L)H_2O]^{0,1-}$ intermediates.

The bicyclic system of TRASUTA retains significant dynamics, despite the conformational constraint imposed by the spiro-fusion, resulting in a lower inertness of the corresponding metal complexes. The flexibility of the spiro-fused system must be considered in the design of mesocyclic chelating agents, in order to obtain metal chelates with improved thermodynamic and kinetic properties.

ASSOCIATED CONTENT

Supporting Information

The Supporting Information is available free of charge at https://pubs.acs.org/doi/10.1021/acs.inorgchem.4c01413.

Experimental procedures, synthetic methodology, potentiometric and kinetic data, and the 1D and 2D NMR investigation of the [M(TRASUTA)] complexes(PDF)

AUTHOR INFORMATION

Corresponding Authors

Zsolt Baranyai − *Bracco Imaging Spa, Basovizza 34149, Italy;* orcid.org/0000-0001-6844-7974; Phone: +39 0403757842; Email: zsolt.baranyai@bracco.com

Giovanni B. Giovenzana − *Dipartimento di Scienze del Farmaco, Università Degli Studi Del Piemonte Orientale, Novara 28100, Italy;* orcid.org/0000-0001-7117-0347; Phone: +39 0321 375 846/746; Email: giovannibattista.giovenzana@uniupo.it

Authors

Ileana Merdzo − *Bracco Imaging Spa, Basovizza 34149, Italy; Department of Chemical and Pharmaceutical Sciences, University of Trieste, Trieste 34127, Italy;* orcid.org/0000-0002-0575-531X

Fabio Travagin − *Dipartimento di Scienze del Farmaco, Università Degli Studi Del Piemonte Orientale, Novara 28100, Italy;* orcid.org/0000-0003-3003-989X

Mariangela Boccalon − *Bracco Imaging Spa, Basovizza 34149, Italy*

Enzo Alessio − *Department of Chemical and Pharmaceutical Sciences, University of Trieste, Trieste 34127, Italy;* orcid.org/0000-0002-4908-9400

Luciano Lattuada − *Bracco Imaging Spa, Bracco Research Centre, Colleretto Giacosa 10010, Italy*

Complete contact information is available at: https://pubs.acs.org/10.1021/acs.inorgchem.4c01413

Author Contributions

The manuscript was written with the contributions of all authors. All authors have given approval to the final version of the manuscript.

Notes

The authors declare no competing financial interest.

TRASUTA: 1,7,10-TRiAzaSpiro[4.6]-Undecane-1,7,10-TriAcetic acid.

ACKNOWLEDGMENTS

This publication is part of the project NODES which has received funding from the MUR—M4C2 1.5 of PNRR with grant agreement no. ECS00000036 (G.B.G., F.T.). The DM 352 PhD scholarship of IM (code 38-033-33-DOT1333997-2791) was co-financed by Bracco Imaging SpA and MUR-PNRR (CUP J92B22001010007).

REFERENCES

(1) Hart, J. R. Ethylenediaminetetraacetic Acid and Related Chelating Agents. *Ullmann's Encyclopedia of Industrial Chemistry*; Wiley-VCH, 2011.

(2) Wahsner, J.; Gale, E. M.; Rodríguez-Rodríguez, A.; Caravan, P. Chemistry of MRI Contrast Agents: Current Challenges and New Frontiers. *Chem. Rev.* **2019**, *119* (2), 957−1057.

(3) Wadas, T. J.; Wong, E. H.; Weisman, G. R.; Anderson, C. J. Coordinating Radiometals of Copper, Gallium, Indium, Yttrium, and Zirconium for PET and SPECT Imaging of Disease. *Chem. Rev.* **2010**, *110* (5), 2858−2902.
(4) Kostelnik, T. I.; Orvig, C. Radioactive Main Group and Rare Earth Metals for Imaging and Therapy. *Chem. Rev.* **2019**, *119* (2), 902−956.
(5) Boros, E.; Packard, A. B. Radioactive Transition Metals for Imaging and Therapy. *Chem. Rev.* **2019**, *119* (2), 870−901.
(6) Grieve, M. L.; Paterson, B. M. The Evolving Coordination Chemistry of Radiometals for Targeted Alpha Therapy. *Aust. J. Chem.* **2021**, *75* (2), 65−88.
(7) Crisponi, G.; Nurchi, V. M. Chapter 2—Chelating Agents as Therapeutic Compounds—Basic Principles. *Chelation Therapy in the Treatment of Metal Intoxication*; Aaseth, J., Crisponi, G., Andersen, O., Eds.; Academic Press: Boston, 2016; pp 35−61.
(8) Delgado, R.; Félix, V.; Lima, L. M. P.; Price, D. W. Metal Complexes of Cyclen and Cyclam Derivatives Useful for Medical Applications: A Discussion Based on Thermodynamic Stability Constants and Structural Data. *Dalton Trans.* **2007**, *26*, 2734−2745.
(9) Jackson, J. A.; Hungnes, I. N.; Ma, M. T.; Rivas, C. Bioconjugates of Chelators with Peptides and Proteins in Nuclear Medicine: Historical Importance, Current Innovations, and Future Challenges. *Bioconjugate Chem.* **2020**, *31* (3), 483−491.
(10) Waldron, B. P.; Parker, D.; Burchardt, C.; Yufit, D. S.; Zimny, M.; Roesch, F. Structure and Stability of Hexadentate Complexes of Ligands Based on AAZTA for Efficient PET Labelling with Gallium-68. *Chem. Commun.* **2013**, *49* (6), 579−581.
(11) Aime, S.; Calabi, L.; Cavallotti, C.; Gianolio, E.; Giovenzana, G. B.; Losi, P.; Maiocchi, A.; Palmisano, G.; Sisti, M. [Gd-AAZTA]-: A New Structural Entry for an Improved Generation of MRI Contrast Agents. *Inorg. Chem.* **2004**, *43* (24), 7588−7590.
(12) Nagy, G.; Szikra, D.; Trencsényi, G.; Fekete, A.; Garai, I.; Giani, A. M.; Negri, R.; Masciocchi, N.; Maiocchi, A.; Uggeri, F.; Tóth, I.; Aime, S.; Giovenzana, G. B.; Baranyai, Z. AAZTA: An Ideal Chelating Agent for the Development of 44Sc PET Imaging Agents. *Angew Chem Int Ed Engl.* **2017**, *56* (8), 2118−2122.
(13) Baranyai, Z.; Uggeri, F.; Maiocchi, A.; Giovenzana, G. B.; Cavallotti, C.; Takács, A.; Tóth, I.; Bányai, I.; Bényei, A.; Brucher, E.; Aime, S. Equilibrium, Kinetic and Structural Studies of AAZTA Complexes with Ga^{3+}, In^{3+} and Cu^{2+}. *Eur. J. Inorg. Chem.* **2013**, *2013* (1), 147−162.
(14) Kálmán, F. K.; Tircsó, G. Kinetic Inertness of the Mn2+ Complexes Formed with AAZTA and Some Open-Chain EDTA Derivatives. *Inorg. Chem.* **2012**, *51* (19), 10065−10067.
(15) Baranyai, Z.; Uggeri, F.; Giovenzana, G. B.; Bényei, A.; Brücher, E.; Aime, S. Equilibrium and Kinetic Properties of the Lanthanoids-(III) and Various Divalent Metal Complexes of the Heptadentate Ligand AAZTA. *Chem.—Eur. J.* **2009**, *15* (7), 1696−1705.
(16) Giovenzana, G. B.; Lattuada, L.; Negri, R. Recent Advances in Bifunctional Paramagnetic Chelates for MRI. *Isr. J. Chem.* **2017**, *57* (9), 825−832.
(17) Lattuada, L.; Barge, A.; Cravotto, G.; Giovenzana, G. B.; Tei, L. The Synthesis and Application of Polyamino Polycarboxylic Bifunctional Chelating Agents. *Chem. Soc. Rev.* **2011**, *40* (5), 3019−3049.
(18) Ghiani, S.; Hawala, I.; Szikra, D.; Trencsényi, G.; Baranyai, Z.; Nagy, G.; Vágner, A.; Stefania, R.; Pandey, S.; Maiocchi, A. Synthesis, Radiolabeling, and Pre-Clinical Evaluation of [44Sc]Sc-AAZTA Conjugate PSMA Inhibitor, a New Tracer for High-Efficiency Imaging of Prostate Cancer. *Eur. J. Nucl. Med. Mol. Imaging* **2021**, *48* (8), 2351−2362.
(19) Greifenstein, L.; Grus, T.; Nagel, J.; Sinnes, J. P.; Rösch, F. Synthesis and Labeling of a Squaric Acid Containing PSMA-Inhibitor Coupled to AAZTA5 for Versatile Labeling with ^{44}Sc, ^{64}Cu, ^{68}Ga and ^{177}Lu. *Appl. Radiat. Isot.* **2020**, *156*, 108867.
(20) Orteca, G.; Sinnes, J.-P.; Rubagotti, S.; Iori, M.; Capponi, P. C.; Piel, M.; Rösch, F.; Ferrari, E.; Asti, M. Gallium-68 and Scandium-44 Labelled Radiotracers Based on Curcumin Structure Linked to Bifunctional Chelators: Synthesis and Characterization of Potential PET Radiotracers. *J. Inorg. Biochem.* **2020**, *204*, 110954.
(21) Sinnes, J.-P.; Nagel, J.; Rösch, F. AAZTA5/AAZTA5-TOC: Synthesis and Radiochemical Evaluation with ^{68}Ga, ^{44}Sc and ^{177}Lu. *EJNMMI radiopharm. chem.* **2019**, *4* (1), 18.
(22) Pfister, J.; Summer, D.; Rangger, C.; Petrik, M.; von Guggenberg, E.; Minazzi, P.; Giovenzana, G. B.; Aloj, L.; Decristoforo, C. Influence of a Novel, Versatile Bifunctional Chelator on Theranostic Properties of a Minigastrin Analogue. *EJNMMI Res.* **2015**, *5* (1), 74.
(23) Manzoni, L.; Belvisi, L.; Arosio, D.; Bartolomeo, M. P.; Bianchi, A.; Brioschi, C.; Buonsanti, F.; Cabella, C.; Casagrande, C.; Civera, M.; De Matteo, M.; Fugazza, L.; Lattuada, L.; Maisano, F.; Miragoli, L.; Neira, C.; Pilkington-Miksa, M.; Scolastico, C. Synthesis of Gd and 68Ga Complexes in Conjugation with a Conformationally Optimized RGD Sequence as Potential MRI and PET Tumor-Imaging Probes. *ChemMedChem* **2012**, *7* (6), 1084−1093.
(24) Gianolio, E.; Cabella, C.; Colombo Serra, S.; Valbusa, G.; Arena, F.; Maiocchi, A.; Miragoli, L.; Tedoldi, F.; Uggeri, F.; Visigalli, M.; Bardini, P.; Aime, S. B25716/1: A Novel Albumin-Binding Gd-AAZTA MRI Contrast Agent with Improved Properties in Tumor Imaging. *J. Biol. Inorg. Chem.* **2014**, *19* (4−5), 715−726.
(25) Liu, X.; Chen, L.; Li, Y.; He, C.; Zhang, X.; Zhou, H.; Bao, G.; Zhu, X.; Xiang, G.; Ma, X. Synthesis of Novel DOTA-/AAZTA-Based Bifunctional Chelators: Solution Thermodynamics, Peptidomimetic Conjugation, and Radiopharmaceutical Evaluation. *Biomed. Pharmacother.* **2023**, *165*, 115114.
(26) Hennrich, U.; Benešová, M. [68Ga]Ga-DOTA-TOC: The First FDA-Approved 68Ga-Radiopharmaceutical for PET Imaging. *Pharmaceuticals* **2020**, *13* (3), 38.
(27) Viswanathan, R.; Ballal, S.; Yadav, M. P.; Roesch, F.; Sheokand, P.; Satapathy, S.; Tripathi, M.; Agarwal, S.; Moon, E. S.; Bal, C. Head-to-Head Comparison of SSTR Antagonist [68Ga]Ga-DATA5m-LM4 with SSTR Agonist [68Ga]Ga-DOTANOC PET/CT in Patients with Well Differentiated Gastroenteropancreatic Neuroendocrine Tumors: A Prospective Imaging Study. *Pharmaceuticals* **2024**, *17* (3), 275.
(28) Greifenstein, L.; Kramer, C. S.; Moon, E. S.; Rösch, F.; Klega, A.; Landvogt, C.; Müller, C.; Baum, R. P. From Automated Synthesis to In Vivo Application in Multiple Types of Cancer—Clinical Results with [68Ga]Ga-DATA5m.SA.FAPi. *Pharmaceuticals* **2022**, *15* (8), 1000.
(29) Travagin, F.; Lattuada, L.; Giovenzana, G. B. AAZTA: The Rise of Mesocyclic Chelating Agents for Metal Coordination in Medicine. *Coord. Chem. Rev.* **2021**, *438*, 213908−213931.
(30) Martinelli, J.; Martorana, E.; Tei, L. Synthesis of a Rigidified Bicyclic AAZTA-like Ligand and Relaxometric Characterization of Its GdIII Complex. *Tetrahedron Lett.* **2020**, *61* (48), 152573.
(31) Farkas, E.; Vágner, A.; Negri, R.; Lattuada, L.; Tóth, I.; Colombo, V.; Esteban-Gómez, D.; Platas-Iglesias, C.; Notni, J.; Baranyai, Z.; Giovenzana, G. B. PIDAZTA: Structurally Constrained Chelators for the Efficient Formation of Stable Gallium-68 Complexes at Physiological pH. *Chem.—Eur. J.* **2019**, *25* (45), 10698−10709.
(32) Vágner, A.; Gianolio, E.; Aime, S.; Maiocchi, A.; Tóth, I.; Baranyai, Z.; Tei, L. High Kinetic Inertness of a Bis-Hydrated Gd-Complex with a Constrained AAZTA-like Ligand. *Chem. Commun.* **2016**, *52* (75), 11235−11238.
(33) Vágner, A.; D'Alessandria, C.; Gambino, G.; Schwaiger, M.; Aime, S.; Maiocchi, A.; Tóth, I.; Baranyai, Z.; Tei, L. A Rigidified AAZTA-like Ligand as Efficient Chelator for 68Ga Radiopharmaceuticals. *ChemistrySelect* **2016**, *1* (2), 163−171.
(34) Irving, H. M.; Miles, M. G.; Pettit, L. D. A Study of Some Problems in Determining the Stoicheiometric Proton Dissociation Constants of Complexes by Potentiometric Titrations Using a Glass Electrode. *Anal. Chim. Acta* **1967**, *38*, 475−488.
(35) Zekany, L.; Nagypal, I. PSEQUAD. *Computational Methods for the Determination of Formation Constants*; Leggett, D. J., Ed.; Modern Inorganic Chemistry; Springer US: Boston, MA, 1985; pp 291−353.

(36) Oe, H.; Takahashi, N.; Doi, E.; Hirose, M. Effects of Anion Binding on the Conformations of the Two Domains of Ovotransferrin. *J. Biochem.* **1989**, *106* (5), 858−863.
(37) Noble, A.; Anderson, J. C. Nitro-Mannich Reaction. *Chem. Rev.* **2013**, *113* (5), 2887−2939.
(38) Farkas, E.; Nagel, J.; Waldron, B. P.; Parker, D.; Tóth, I.; Brücher, E.; Rösch, F.; Baranyai, Z. Equilibrium, Kinetic and Structural Properties of Gallium(III) and Some Divalent Metal Complexes Formed with the New DATAm and DATA5m Ligands. *Chem.—Eur. J.* **2017**, *23* (43), 10358−10371.
(39) Motekaitis, R. J.; Martell, A. E. Gallium Complexes of Multidentate Ligands in Aqueous Solution. *Inorg. Chem.* **1980**, *19* (6), 1646−1651.
(40) Delgado, R.; Sun, Y.; Motekaitis, R. J.; Martell, A. E. Stabilities of Divalent and Trivalent Metal Ion Complexes of Macrocyclic Triazatriacetic Acids. *Inorg. Chem.* **1993**, *32* (15), 3320−3326.
(41) Geraldes, C. F. G. C.; Delgado, R.; Urbano, A. M.; Costa, J.; Jasanada, F.; Nepveu, F. Complexes of Ga^{3+} and In^{3+} with the N,N″-Bis(Butylamide) Derivative of Diethylenetriaminepentaacetic Acid: Stability Constants and Nuclear Magnetic Resonance Studies in Aqueous Solution. *J. Chem. Soc., Dalton Trans.* **1995**, No. 3, 327−335.
(42) Baes, C. F.; Mesmer, R. E. *The Hydrolysis of Cations*; Wiley: New York, 1976.
(43) Akitt, J. W.; Kettle, D. ^{71}Ga Nuclear Magnetic Resonance Investigation of Aqueous Gallium(III) and Its Hydrolysis. *Magn. Reson. Chem.* **1989**, *27* (4), 377−379.
(44) Tóth, I.; Zékány, L.; Brücher, E. Equilibrium Study of the Systems of Aluminium(III), Gallium(III) and Indium(III) with Mercaptoacetate, 3-Mercaptopropionate and 2-Mercaptobenzoate. *Polyhedron* **1984**, *3* (7), 871−877.
(45) Harris, W. R.; Pecoraro, V. L. Thermodynamic Binding Constants for Gallium Transferrin. *Biochemistry* **1983**, *22* (2), 292−299.
(46) Kubíček, V.; Havlíčková, J.; Kotek, J.; Tircsó, G.; Hermann, P.; Tóth, É.; Lukeš, I. Gallium(III) Complexes of DOTA and DOTA-Monoamide: Kinetic and Thermodynamic Studies. *Inorg. Chem.* **2010**, *49* (23), 10960−10969.
(47) Šimeček, J.; Schulz, M.; Notni, J.; Plutnar, J.; Kubíček, V.; Havlíčková, J.; Hermann, P. Complexation of Metal Ions with TRAP (1,4,7-Triazacyclononane Phosphinic Acid) Ligands and 1,4,7-Triazacyclononane-1,4,7-Triacetic Acid: Phosphinate-Containing Ligands as Unique Chelators for Trivalent Gallium. *Inorg. Chem.* **2012**, *51* (1), 577−590.
(48) Broan, C. J.; Cox, J. P. L.; Craig, A. S.; Kataky, R.; Parker, D.; Harrison, A.; Randall, A. M.; Ferguson, G. Structure and Solution Stability of Indium and Gallium Complexes of 1,4,7-Triazacyclononanetriacetate and of Yttrium Complexes of 1,4,7,10-Tetraazacyclododecanetetraacetate and Related Ligands: Kinetically Stable Complexes for Use in Imaging and Radioimmunotherapy. X-Ray Molecular Structure of the Indium and Gallium Complexes of 1,4,7-Triazacyclononane-1,4,7-Triacetic Acid. *J. Chem. Soc., Perkin Trans. 2* **1991**, *2* (1), 87−99.
(49) Li, Y.; Liu, B.; Ge, Z.; Yang, B. Spectroscopic Analysis of the Interaction between Gallium(III) and Apoovotransferrin. *J. Photochem. Photobiol., B* **2008**, *91* (2−3), 137−142.
(50) Parker, D.; Waldron, B. P.; Yufit, D. S. Crystallographic and Solution NMR Structural Analyses of Four Hexacoordinated Gallium(Iii) Complexes Based on Ligands Derived from 6-Amino-Perhydro-1,4-Diazepine. *Dalton Trans.* **2013**, *42* (22), 8001−8008.
(51) Aime, S.; Bombieri, G.; Cavallotti, C.; Giovenzana, G. B.; Imperio, D.; Marchini, N. An unusual gadolinium ten-coordinated dimeric complex in the series of MRI contrast agents: Na[Gd(H_2O)-AAZTA]·3H_2O. *Inorg. Chim. Acta* **2008**, *361* (5), 1534−1541.
(52) Day, R. J.; Reilley, C. N. Nuclear Magnetic Resonance Studies of Metal Aminopolycarboxylate Complexes. Lability of Individual Metal Ligand Bonds in (Ethylenedinitrilo)-Tetraacetate Complexes. *Anal. Chem.* **1964**, *36* (6), 1073−1076.
(53) Day, R. J.; Reilley, C. N. Nuclear Magnetic Resonance Studies of Metal Aminopolycarboxylate Complexes. Structural Effects on the Labilities of Individual Metal-Ligand Bonds. *Anal. Chem.* **1965**, *37* (11), 1326−1333.
(54) Jószai, R.; Purgel, M.; Pápai, I.; Wakita, H.; Tóth, I. Multinuclear NMR and DFT Studies of the Structure and Fluxionality for M^{III}-Ethylenediamine-Tetraacetate Complexes ($M(EDTA)^-$, M = Al, Ga and In) in Solution. *J. Mol. Liq.* **2007**, *131−132*, 72−80.
(55) Polynova, T. N.; Filippova, T. V.; Porai-Koshits, M. A.; Belskii, V. K.; Sobolev, A. N.; Myachina, L. I. *Koord. Khim.* **1988**, *14*, 405.
(56) Fuertes, A.; Miravitlles, C.; Escriva, E.; Coronado, E.; Beltran, D.; Padel, L. J. Bimetallic compounds of trans-cyclohexane-1,2-diamine-NNN′N′-tetra-acetate (cdta). Part 3. Structural and magnetic characterization of the dinuclear $[M(OH_2)_5]$ $[M'(cdta)]\cdot H_2O$ (M,M′= Ni,Ni; Mn,Ni; Mn,Cu; Co,Ni; or Co,Cu) and the tetranuclear $[M(OH_2)_4]$ $[M'(cdta)(OH_2)]\cdot 4H_2O$ (M,M′= Zn,Zn; Zn−Co; Co,Co; or Mn,Co) complexes. *J. Chem. Soc., Dalton Trans.* **1989**, 863.